Electronic supplementary information

Dual potassium salts-assisted lyophilization of natural fibres for high-yield synthesis of one-dimensional carbon microtubes for supercapacitor and oxygen reduction reaction

Jiawei Qi, Wendu Zhang, Haozhi Zhou and Lang Xu*

MOE Key Laboratory of Coal Processing and Efficient Utilization, School of Chemical Engineering and Technology, China University of Mining and Technology, 1 Daxue Road, Xuzhou, Jiangsu, 221116, China

*Corresponding author. *E-mail address: lang.xu@cumt.edu.cn* (L. Xu)

Table S1 Segmented specific surface areas and pore volumes of CMTs based on the DFT model.[a]

CMT	S_{DFT} ($m^2\ g^{-1}$)	$S_{0–0.7nm}$ ($m^2\ g^{-1}$)	$S_{0.7–2nm}$ ($m^2\ g^{-1}$)	$S_{2–50nm}$ ($m^2\ g^{-1}$)	V_{DFT} ($cm^3\ g^{-1}$)	$V_{0–0.7nm}$ ($cm^3\ g^{-1}$)	$V_{0.7–2nm}$ ($cm^3\ g^{-1}$)	$V_{2–50nm}$ ($cm^3\ g^{-1}$)
KCMT*-12*-700	1979.5	1464.4	515.1	0	0.627	0.394	0.234	0
KCMT*-12*-800	1920.5	899.2	803.5	217.8	0.771	0.243	0.381	0.150
KCMT*-12*-900	1625.8	115.4	657.7	852.7	1.387	0.025	0.367	0.995
PCMT*-12*-800	1982.4	811.2	693.8	477.4	0.962	0.198	0.341	0.423
CCMT*-12*-800	2027.2	1172.8	744.9	109.5	0.734	0.306	0.334	0.094

[a] S_{DFT}: DFT specific surface area; $S_{0–0.7nm}$: specific surface area of micropores with width of 0–0.7 nm; $S_{0.7–2nm}$: specific surface area of micropores with width of 0.7–2 nm; $S_{2–50nm}$: specific surface area of mesopores; V_{DFT}: DFT total pore volume; $V_{0–0.7nm}$: pore volume of micropores with width of 0–0.7 nm; $V_{0.7–2nm}$: pore volume of micropores with width of 0.7–2 nm; $V_{2–50nm}$: pore volume of mesopores.

Table S2 Surface composition parameters of KCMTs and N_{ox}-KCMT.

CMT	C at%	N at%	O at%	N-6 %	N-5 %	N-Q %	N-O %
$KCMT_{12}$-700	87.96	0.85	11.19	13.34	27.83	29.91	28.92
$KCMT_{12}$-800	91.41	0.77	7.82	2.82	55.50	20.95	20.73
$KCMT_{12}$-900	92.70	1.21	6.09	14.99	43.76	21.82	19.43
N_{ox}-KCMT	88.81	2.59	8.60	24.49	44.22	23.50	7.79

Fig. S1 A schematic illustration of the preparation procedure of KCMT and N_{ox}-KCMT.

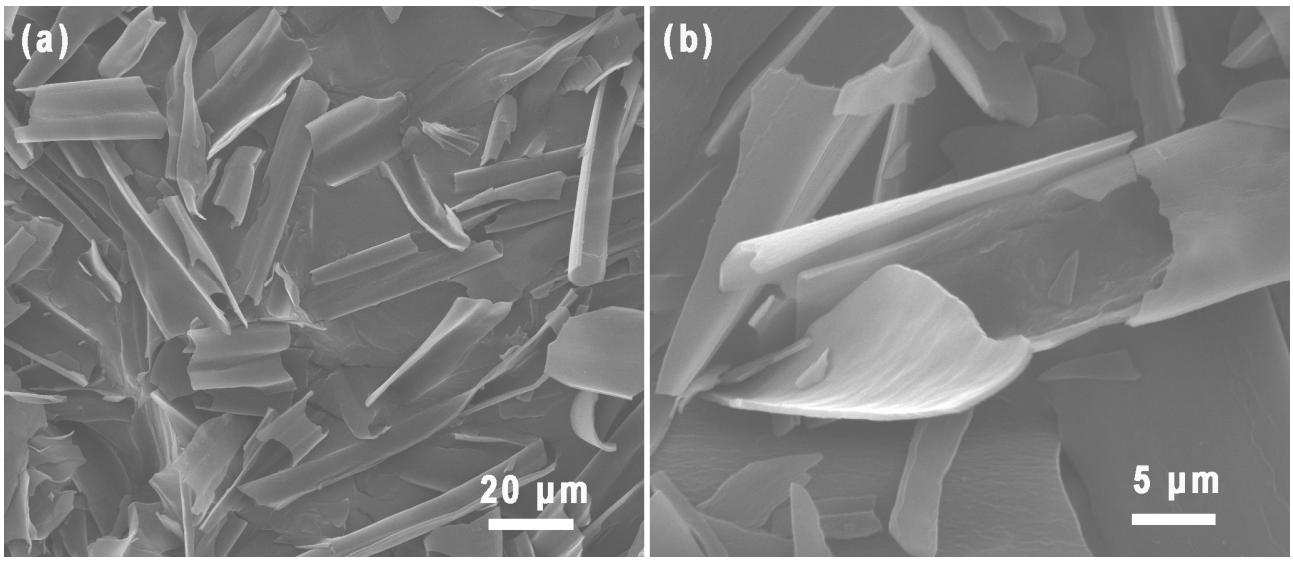

Fig. S2 (a, b) SEM images of KCMT$_1$-800 at different magnifications.

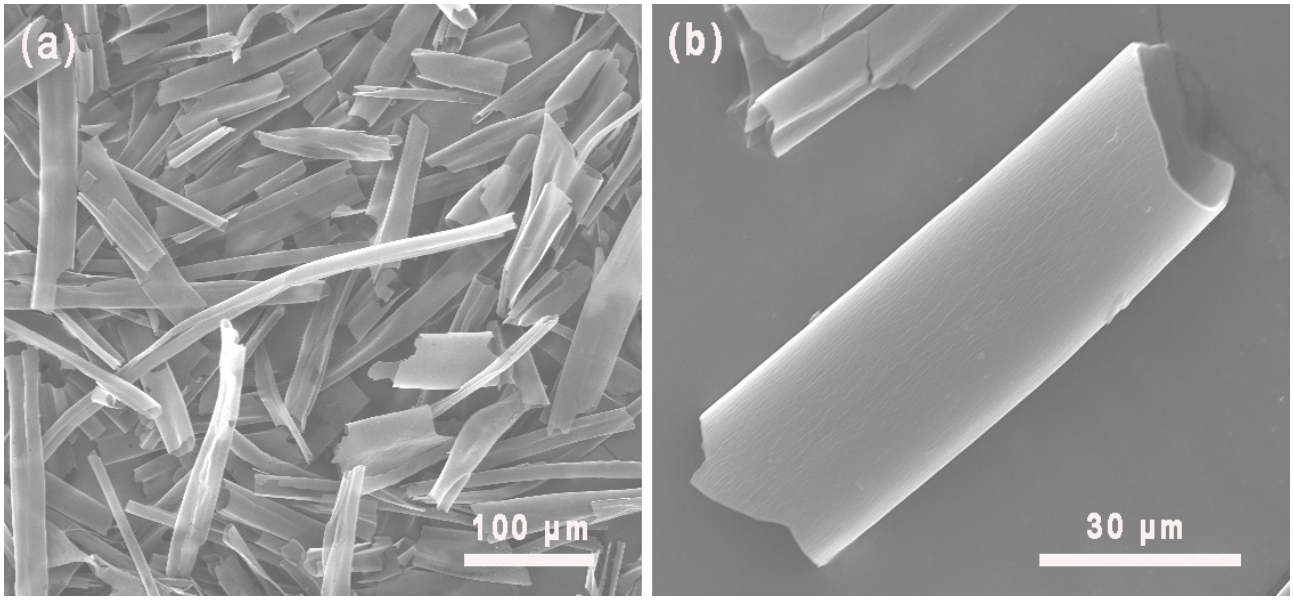

Fig. S3 (a, b) SEM images of KCMT$_2$-800 at different magnifications.

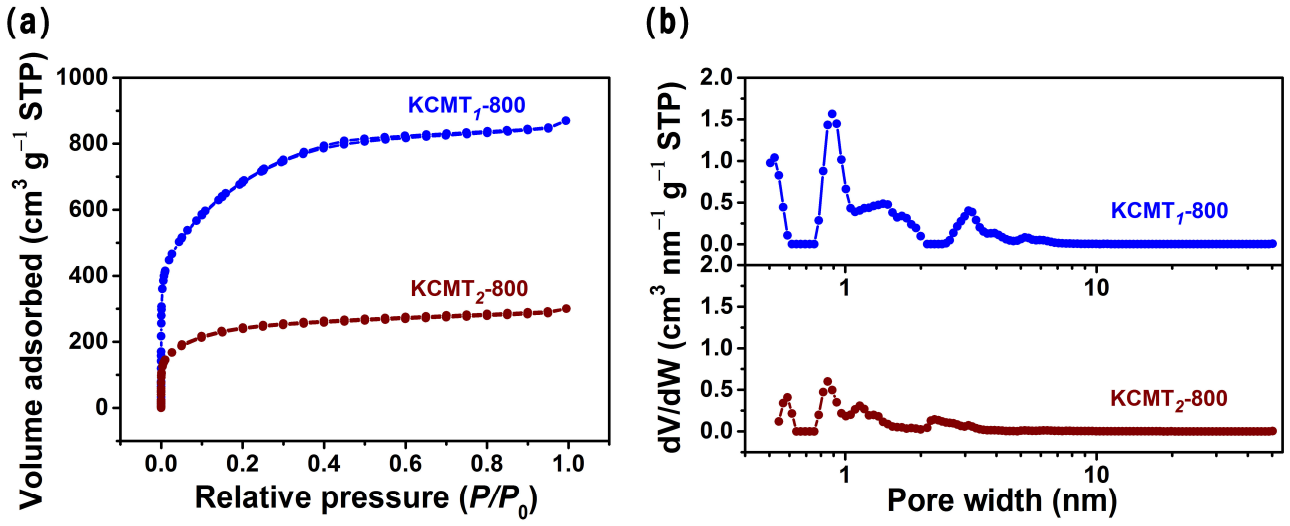

Fig. S4 (a) N_2 adsorption/desorption isotherms of KCMT$_1$-800 and KCMT$_2$-800, (b) pore width distribution curves of KCMT$_1$-800 and KCMT$_2$-800 based on the DFT model.

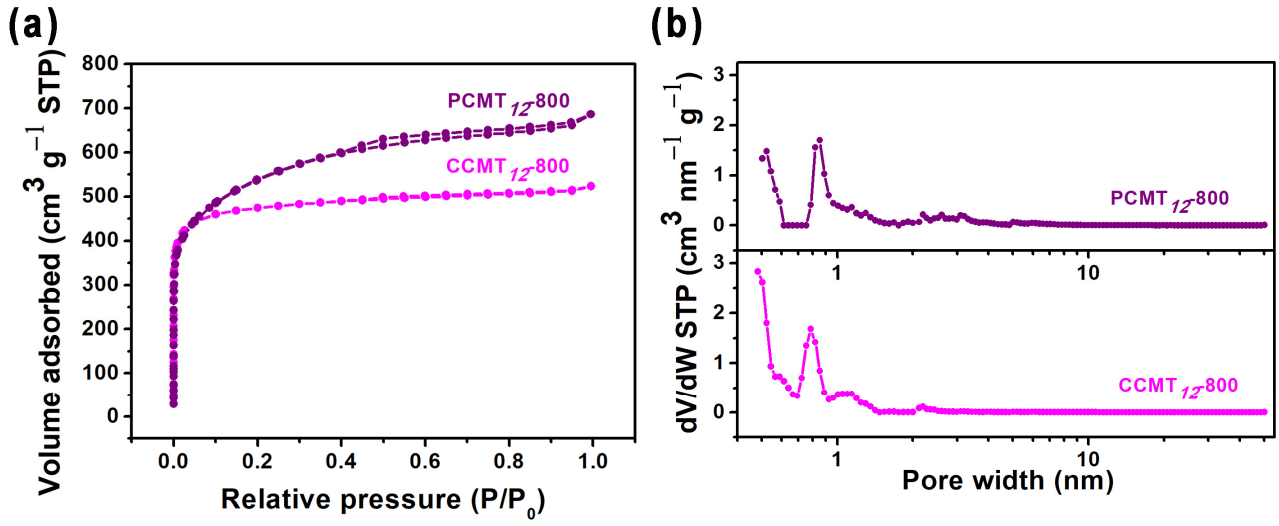

Fig. S5 (a) N_2 adsorption/desorption isotherms of PCMT$_{12}$-800 and CCMT$_{12}$-800; (b) pore width distribution curves of PCMT$_{12}$-800 and CCMT$_{12}$-800 based on the DFT model.

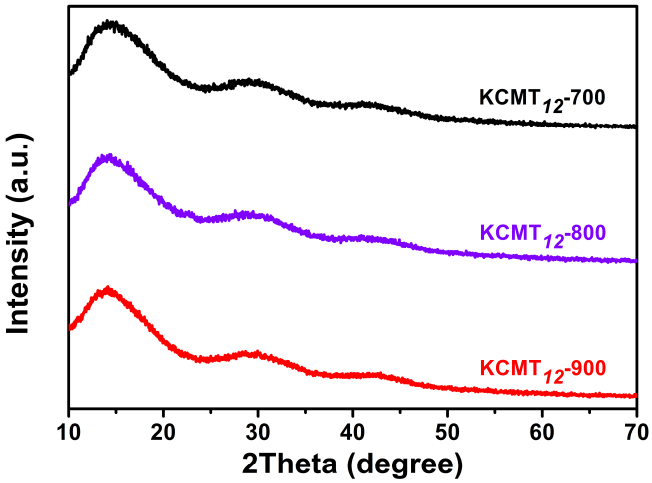

Fig. S6 XRD patterns of KCMT$_{12}$-700, KCMT$_{12}$-800 and KCMT$_{12}$-900.

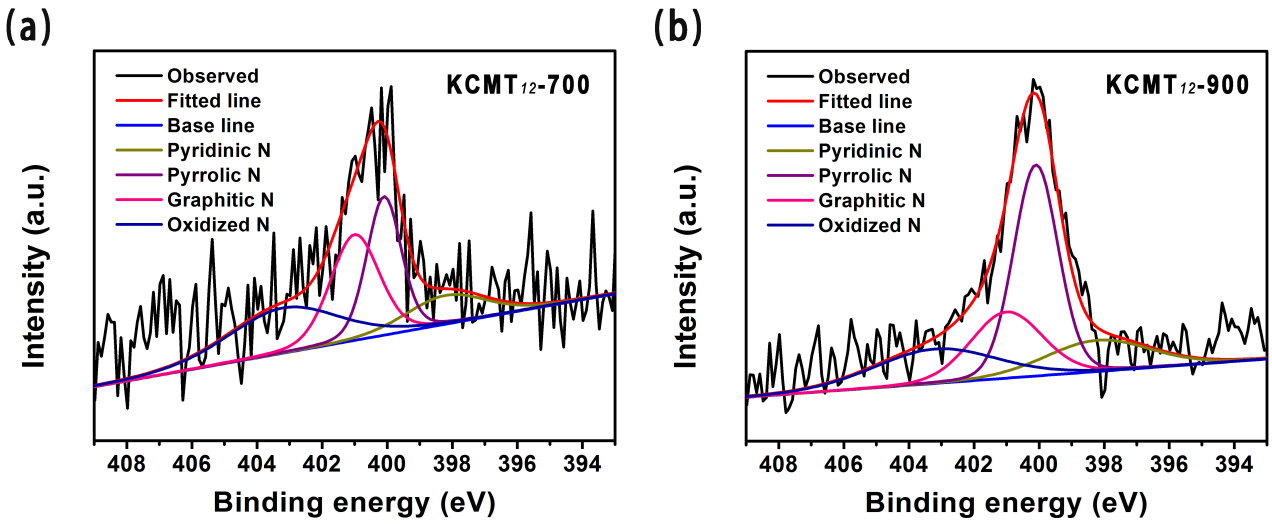

Fig. S7 (a) High-resolution of N 1s spectrum of KCMT$_{12}$-700; (b) high-resolution of N 1s spectrum of KCMT$_{12}$-900.

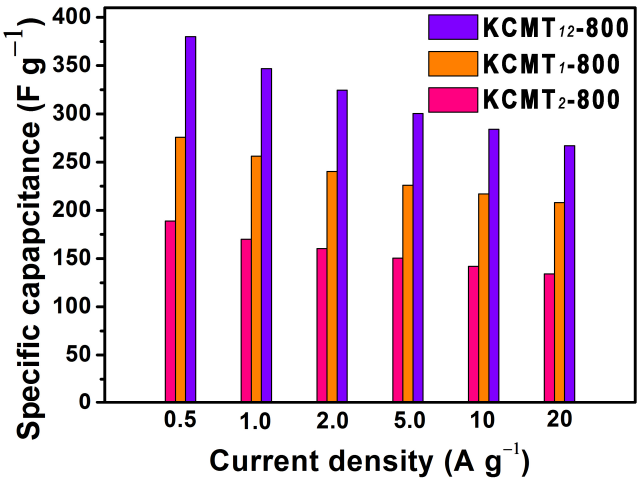

Fig. S8 Specific capacitances of KCMT$_2$-800, KCMT$_1$-800 and KCMT$_{12}$-800 at different current densities.

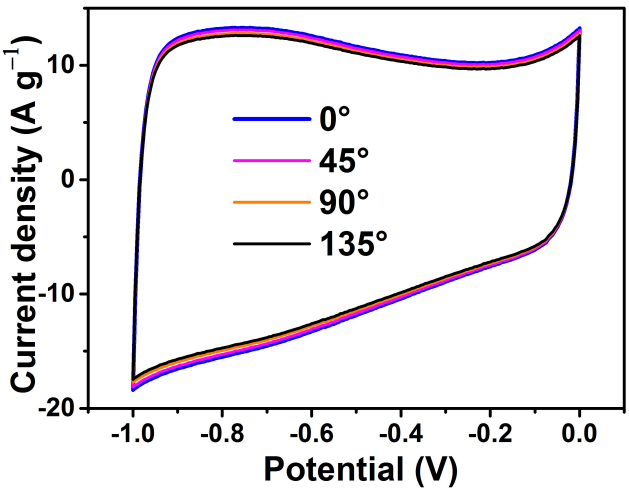

Fig. S9 CV curves in different bending conditions at a scan rate of 50 mV s^{-1}.

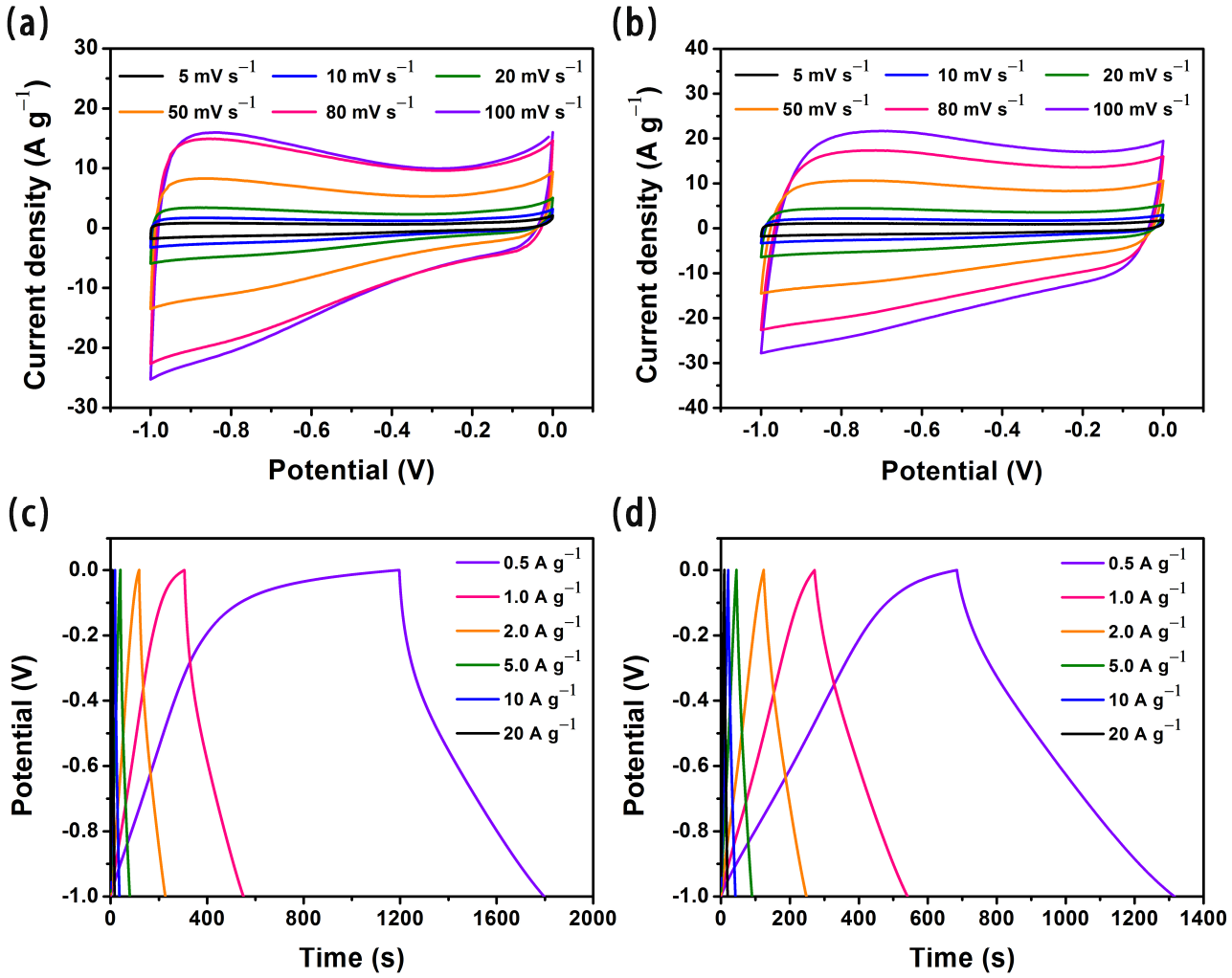

Fig. S10 (a) CV curves of PCMT$_{12}$-800 at different scan rates; (b) CV curves of CCMT$_{12}$-800 at different scan rates; (c) GCD curves of PCMT$_{12}$-800 at different charge/discharge current densities; (d) GCD curves of CCMT$_{12}$-800 at different charge/discharge current densities. All the measurements were taken in 6 M KOH in 25 °C.

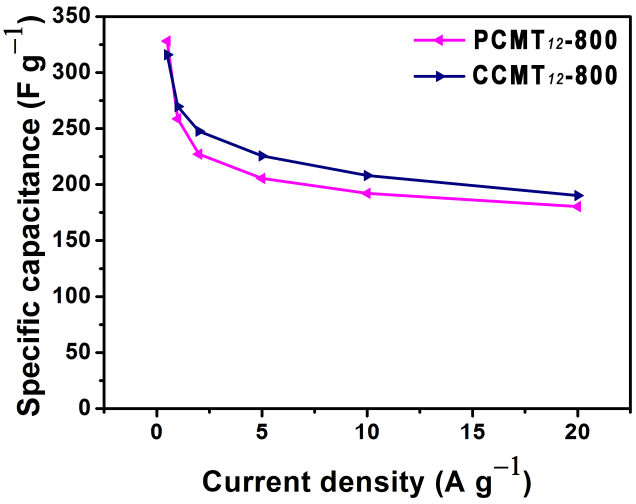

Fig. S11 Specific capacitances of PCMT$_{12}$-800 and CCMT$_{12}$-800 at different current densities.

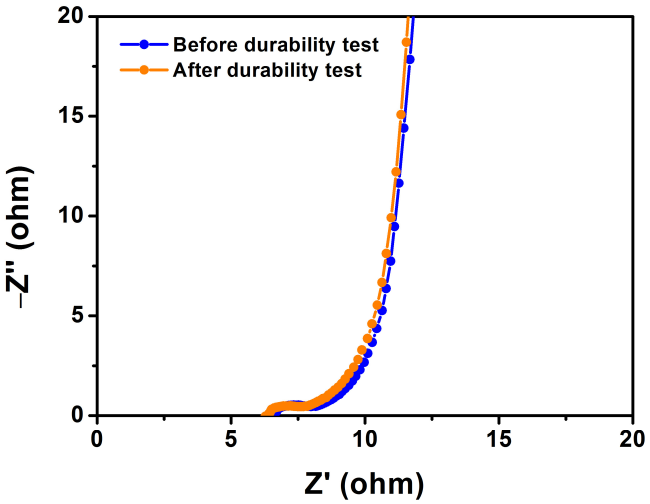

Fig. S12 Nyquist plots of KCMT$_{12}$-800//KCMT$_{12}$-800 in a frequency range from 10^{5} to 10^{-2} Hz with 10 mV AC amplitude at an open circuit potential before and after durability test (2 M Li_2SO_4 electrolyte).

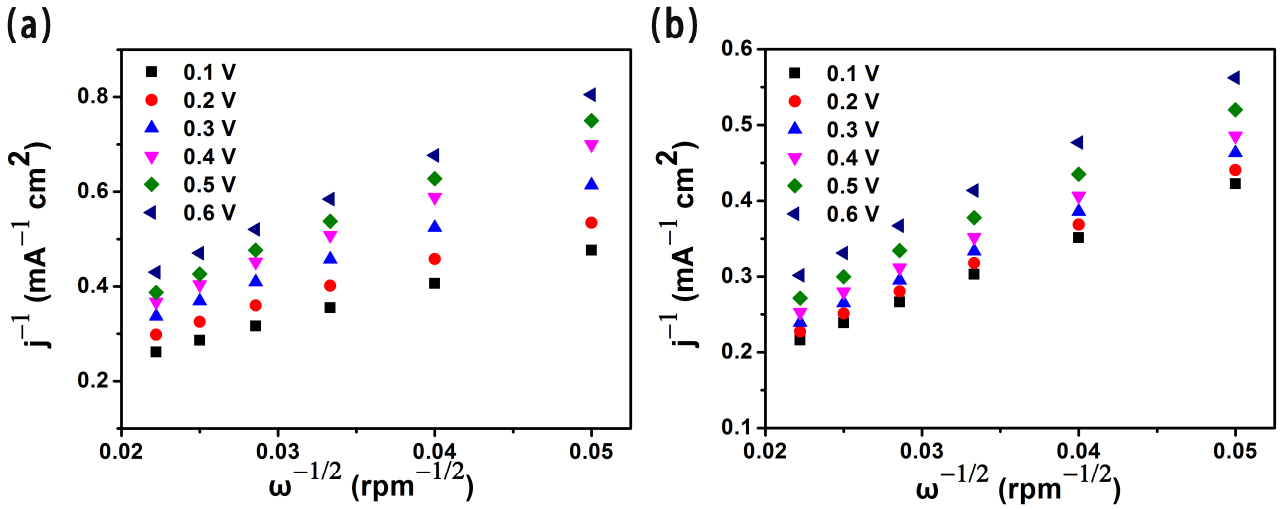

Fig. S13 (a) The K–L plots of KCMT$_{12}$-800; (b) the K–L plots of N-KCMT.